PHILOSOPHICAL TRANSACTIONS OF THE ROYAL SOCIETY A MATHEMATICAL, PHYSICAL & ENGINEERING SCIENCES

# Melting of Mantle and Core Materials at Very High Pressures

R. Boehler

*Phil. Trans. R. Soc. Lond. A* 1996 **354**, 1265-1278
doi: 10.1098/rsta.1996.0048

# Melting of mantle and core materials at very high pressures

By R. Boehler

*Max-Planck-Institut für Chemie, 55020 Mainz, Germany*

Melting experiments on the most important mantle and core materials (Mg-Si-perovskite, magnesiowüstite, iron and its sulphur and oxygen compounds) are reviewed and possible sources of controversies with results from other laboratories are discussed. The iron phase diagram, measured in laser-heated diamond cells to 2 Mbar, may be reconciled with shock sound velocity measurements if one allows a correction of about 1000 K for the overshoot of equilibrium conditions during shock. The data suggest a new, yet unidentified, phase for the inner core and an inner-core temperature of about 5000 K. The addition of the light elements oxygen and sulphur does not seem to effect the melting temperature of pure iron at very high pressure.

The melting curves of the major lower-mantle minerals Mg-Si-perovskite and magnesiowüstite are in sharp contrast to previous estimates. Magnesiowüstite is the low melting phase of the lower mantle but its melting temperature at the core–mantle boundary of about 5000 K is still about twice the average mantle temperature. Even a large temperature increment at the base of the lower mantle, estimated to be at least 1300 K, will not result in melting in the core–mantle boundary region.

## 1. Introduction

Probably no single issue in Earth science has drawn more attention to both theoreticians and experimentalists than the melting phase diagram of iron because the melting temperature of iron plays a key role in the determination of the temperature in the centre of the Earth. Previous theoretical estimates and long extrapolations from low-pressure data showed extreme variations of over 10 000 K and demonstrated the general difficulty in predicting melting temperatures at high pressure. Moreover, seismically measured sound velocities for the liquid outer core require an addition of about 10% of lighter elements to iron, which could be any combination of silicon, oxygen, sulphur, carbon or hydrogen. The unknown properties of these elements in combination with iron, especially their effect on the melting temperature, further complicate temperature estimates in the Earth's centre.

The last nine years have brought a drastic increase in experimental activities to research the phase diagram of iron but, unfortunately, the increase in the amount of data has seemingly complicated the phase diagram and the closing of the previous large pressure gap between static and shock experiments has demonstrated systematic deviations in the melting curves measured with these two different techniques. At present, it is impossible to construct a phase diagram without disregarding whole data sets.

Here, I will argue that static melting experiments on laser-heated iron in a

*Phil. Trans. R. Soc. Lond.* A (1996) **354**, 1265–1278
*Printed in Great Britain*

diamond-anvil cell provide the highest accuracy in the melting temperatures, are in excellent agreement with each other, and that the phase diagram of iron, measured in the diamond cell, can be reconciled with some shock measurements.

Large controversies exist in the melting behaviour of the major lower-mantle mineral (Mg,Fe)$SiO_3$-perovskite. Estimated melting temperatures from previous experiments and theory for lower-mantle pressures vary by several thousand degrees. For (Mg,Fe)O-magnesiowüstite, the second most abundant mineral in the lower mantle, the pressure dependence of melting has never been measured. These melting temperatures are important for mantle models on chemical differentiation and for rheological–dynamical models, because the viscosity most likely scales with the melting temperature.

## 2. Phase diagram of iron

### (*a*) *Melting curves measured in diamond cells*

In 1986, melting temperatures of resistively heated iron wires were measured to over 400 kbar in the diamond cell (Boehler 1986) using a method shown 10 years earlier (Liu & Bassett 1975). New technologies to measure temperatures in the diamond cell using Planck's radiation function to analyse emission spectra over large spectral ranges of the heated sample, measured with diode arrays, had become available. The pyrometric techniques used by Liu & Bassett (1975) to measure temperatures only provided qualitative results on the pressure dependence of melting. The absolute temperature had to be estimated using low-pressure melting data due to the unknown emissivity of the sample. The resistive heating of wires in a diamond cell provided uniform and stable temperatures in large portions of the wire and thus simple optical means to measure the emission spectrum avoiding problems associated with large temperature gradients. Phase transitions and melting could be easily detected by the change of electrical resistivity.

Williams *et al.* (1987) published first data on laser-heated iron samples adopting techniques developed by Ming & Bassett (1974). Unfortunately, the results of Boehler (1986) and Williams *et al.* (1987) were in stark disagreement with each other, showing temperature differences of over 1000 K. Although the pressure range in these early experiments by Williams *et al.* (1987) was doubled, the techniques used to measure temperature and to monitor melting resulted in rather large uncertainties. The early lasers were highly unstable and limited in power, which required tight focussing of the laser beam, resulting in extremely small hotspots with large temperature gradients and fluctuations. Williams *et al.* (1987) collected spectra from areas that were at least 500 times the size of the melt zone. This method required calculation of peak temperatures from average temperatures. Regarding the extreme temperature gradients in such an experiment of about 1000 K $\mu m^{-1}$, uncertainties in such calculations inevitably lead to large errors. Furthermore, standard microscope optics were used, which distort the emission spectra. If the cross section of the hotspot is small or equal to the chromatic aberration of the optical system (e.g. the microscope objective used in their system), temperatures are likely to be overestimated by a large amount (Boehler & Chopelas 1992).

This led Boehler *et al.* (1990) to remeasure the melting curve of iron to over 1 Mbar using improved laser-heating techniques and new methods to measure melting *in situ* and to measure and analyse emission spectra. Problems associated with temperature

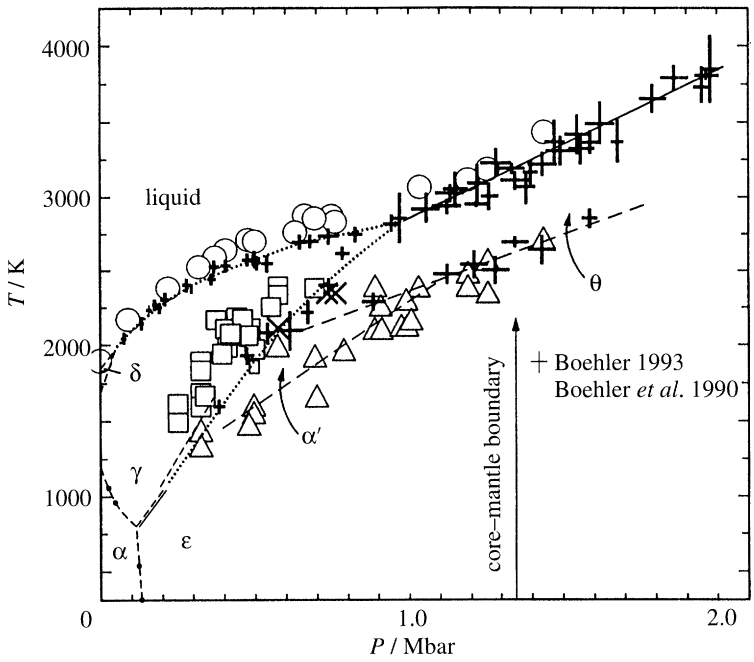


Figure 1. Phase diagram of iron measured in the diamond cell. Bold crosses are from Boehler (1993). Open symbols are from Saxena *et al.* (1994). Circles are melting, squares are $\gamma$-phase boundary, triangles and X symbols are $\epsilon$–$\alpha'$ or $\epsilon$–$\theta$ transitions.

gradients and chromatic aberration were eliminated by defocussing their more powerful and more stable laser and by measuring temperatures from tiny spots of $\mu$ size, which was much smaller than the melted region, using reflecting optics. Melting was measured *in situ* using a variety of optical methods, which were essentially based on the change of reflectivity of the sample undergoing a phase change. Experimental details are described elsewhere (Boehler *et al.* 1990; Boehler 1993). Their results confirmed the low melting gradient of iron and the slope of the HCP–FCC ($\epsilon$–$\gamma$) transition found earlier, which required a triple point at about 1 Mbar. This triple point prevented any reasonable extrapolation of the melting curve to inner-core pressures because the melting slope above the triple point was unknown. For this reason, Boehler (1993) extended the pressure range of his measurements to 2 Mbar by using new laser technology and established a precise melting slope between 1 and 2 Mbar. Boehler's melting curve was confirmed by Shen *et al.* (1993) to 500 kbar, Yoo *et al.* (1992) to 400 kbar and Saxena *et al.* (1994) to 1.5 Mbar using similar techniques and by Ringwood & Hibberson (1990) at 160 kbar using a multi-anvil press. For clarity, only the results of Boehler (1993) and Saxena *et al.* (1994) are shown in figure 1.

The melting temperatures measured by all four groups (Canberra, Livermore, Uppsala, and Mainz) are in excellent agreement with each other and fall within the experimental uncertainties. The data reported by Saxena *et al.* (1994) are at slightly higher temperatures because they used a correction for the wavelength dependence of emissivity. Boehler (1993) used wavelength-independent emissivities because there is a lack of knowledge for the pressure dependence of this property. Assuming extreme cases for the emissivity-wavelength dependence, the maximum uncertainty in temperature estimates is still within a few hundred degrees. The early measurements by Williams *et al.* (1987) are in drastic contrast to all of these measurements. More

details to explain this discrepancy than those described above have been discussed elsewhere (Boehler *et al.* 1990; Duba 1992, 1994). Because of the large systematic errors, those data will be excluded from further discussion.

### (*b*) *Solid–solid transitions in iron*

The phase diagram shown in figure 1 contains all recent data points from Saxena *et al.* (1994) and from Boehler (1993). The main reason for the data scatter is the difficulty in detecting solid–solid phase transitions in iron because these transitions are accompanied by only weak changes in optical properties.

#### (i) *The $\epsilon$–$\alpha'$ (and/or $\epsilon$–$\theta$) transition in iron*

Saxena *et al.* (1993) and Boehler (1993) independently found changes in optical properties of iron below the melting line which they attributed to a new, yet unknown, phase. Such a high $P$–$T$ phase was suggested by Boehler (1986) based on his earlier wire-heating experiments and shock sound velocity measurements (Brown & McQueen 1986). Further measurements (Saxena *et al.* 1994) on this phase boundary, shown by triangles and X-symbols, confirmed Boehler's data but indicated the possibility of yet another high $P$–$T$ phase of iron ($\alpha'$). In view of the weakness of the property changes measured for these transitions and the possibility of hysteresis and sluggishness, however, one could argue that these two transitions ($\epsilon$–$\alpha'$ and $\epsilon$–$\theta$) may be one and the same. For further discussion, it is important to note that there is a phase boundary ($\epsilon$–$\theta$) that is nearly parallel to the melting curve extending to high pressures.

#### (ii) *The stability field of $\gamma$-iron*

The $\epsilon$–$\gamma$ (and/or the $\alpha'$–$\gamma$ and $\theta$–$\gamma$) phase boundaries were also extended to higher pressures (Shen *et al.* 1993; Boehler 1993). Again these transitions are difficult to detect because of the weak changes in optical properties. For reasons of simplicity and because of the large data scatter, I suggest a stability field of $\gamma$-iron which ends near 1 Mbar and about 2800 K, as reported earlier (Boehler 1993) and confirmed later (Saxena *et al.* 1994). My suggested phase boundaries are indicated by dashed lines in figure 1.

### (*c*) *Extrapolation of the phase diagram of iron above* 2 Mbar

The slope of the melting curve between 1 and 2 Mbar measured by Boehler (1993) is well constrained by a large number of data points and is in good agreement with further measurements to 1.5 Mbar (Saxena *et al.* 1994). Boehler (1993) extrapolated this melting curve to 3.3 Mbar, the pressure at the inner-core boundary, using a linear relationship between the melting temperature and the density. This extrapolation is relatively short because the compression range between 2 and 3.3 Mbar is only about 11%. This leads to a melting temperature of pure iron at the inner-core boundary pressure of 4850 K with an uncertainty of about $\pm$200 K. This uncertainty would be somewhat larger if one would include possible large deviations from the linear $T_{\mathrm{m}}$ versus density relationship and if the emissivity of iron depended strongly on the wavelength. For an extreme case, however, both sources of errors would contribute to the uncertainty by not more than a few hundred degrees.

### (*d*) *Shock wave experiments*

Brown & McQueen (1986) measured sound velocities in shock-wave experiments and observed sharp discontinuities in their data at 2 and 2.4 Mbar, which they as-

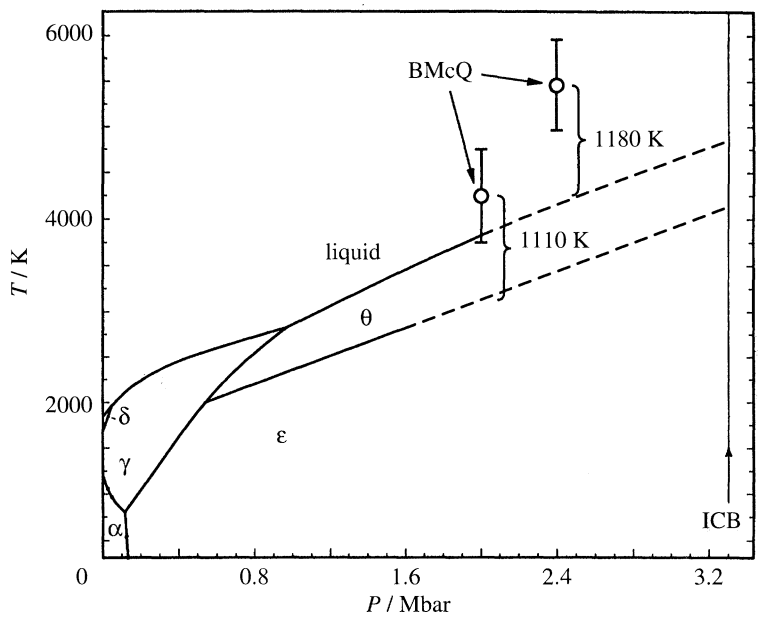


Figure 2. Comparison of the extrapolated phase diagram in figure 1 and shock sound velocity measurements by Brown & McQueen (1986). Both solid–solid and solid–liquid transitions show similar offsets.

signed to the $\epsilon$–$\gamma$ transition and melting, respectively. They calculated the shock temperatures by making assumptions on the specific heat and the Grüneisen parameter. The extreme variation in calculated temperatures in that $P$–$T$ range was reported to be about $\pm 1000$ K. Using a choice of parameters, Brown & McQueen report a melting temperature of $5500 \pm 500$ K at 2.4 Mbar. The temperature gap between the solid–solid transition and melting of about 1000 K, however, depends little on the choice of parameters to calculate shock temperatures. This temperature gap between these two transitions is the same as that obtained from the phase diagram shown in figure 2. It is therefore highly likely that the $P$–$T$ path in the shock experiment crosses the $\epsilon$–$\theta$ transition before it reaches the melting line. Both shock data points are offset by about 1100 K from the phase boundaries shown in figure 2. Considering the higher accuracy in temperature estimates in static melting experiments, I will argue below that the most likely reason for this discrepancy might be an overshoot of the melting line due to the small time scales.

Much larger deviations from static melting measurements are obtained from direct temperature measurements in shock-wave experiments. These shock data (Williams *et al.* 1987; Yoo *et al.* 1993) are shown in figure 3. Static and shock data can only be reconciled by constructing a rather complicated phase diagram. By expanding the error bars of the data by Boehler (1993) and Brown & McQueen (1986), Anderson (1994) constructed a phase diagram by placing a further triple point at 1.9 Mbar near 4100 K. This then deflects the melting curve sharply upwards to satisfy the lower bounds of some of the data points of the Livermore and Caltech shock measurements. Using a Lindemann equation and Brown & McQueen's (1986) solid–liquid point at 2.4 Mbar then yields a melting temperature of iron at the inner-core–outer-core boundary of $6500 \pm 300$ K, about 1700 K higher than that estimated by Boehler (1993). Although Anderson's (1994) solution satisfies to some degree all melting

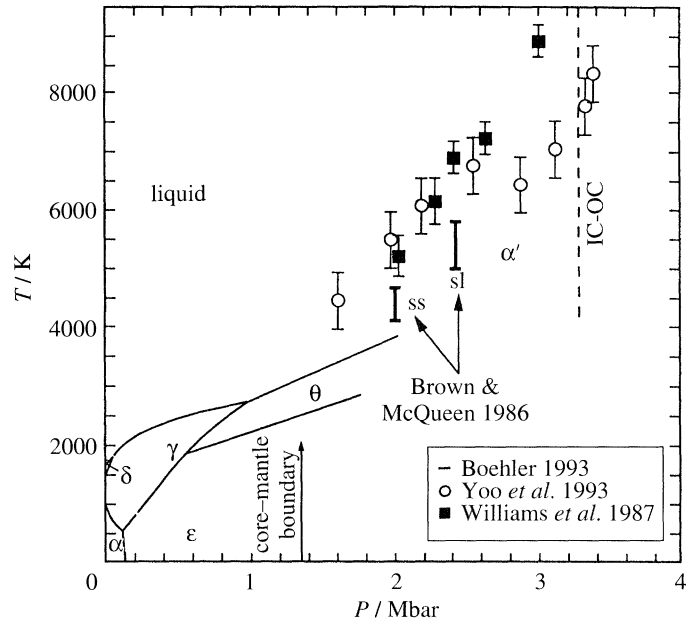


Figure 3. Comparison of the static phase diagram of iron and shock-melting measurements. Reconciliation of all data sets would require an additional triple point near 2 Mbar, an additional phase and a sharp increase in the melting slope.

measurements, it does not take into account the solid–solid phase transition ($\epsilon$–$\theta$) found in diamond-cell experiments (Boehler 1993; Saxena *et al.* 1994). If this phase boundary follows a straight line, as shown in figure 2, and there exists an additional triple point as suggested by Anderson (1994), then Brown & McQueen (1986) should have observed three instead of two discontinuities in their shock sound velocity measurements. The additional discontinuity should have been considerably below 2 Mbar. The problem remains that a phase diagram above 2 Mbar cannot be easily constructed without deleting either sets of static or dynamic measurements.

I have argued here that the total uncertainty in temperature measurements and in the detection of melting in diamond-cell experiments is not more than a few hundred degrees. There are, however, a number of sources of potentially large errors in shock temperature measurements, most of which are purely technical, such as fitting problems associated with the scatter and small number of data to analyse the radiation spectra, sample porosity, and imperfect sample-window bond. Subject to larger systematic errors are the optical and thermal properties (especially thermal conductivity) of the window material. The magnitude of these uncertainties can be approximately estimated and could lead to errors as large as the difference between the static and shock experiments (Duba 1994; Brown, personal communication). Recent measurements on the thermal conductivity of such window materials (Gallagher & Ahrens 1994) have lead to a reduction of temperatures calculated from emission measurements in shock experiments of 1000 K. The fact remains that the measured shock melting temperatures are systematically higher than those measured in static experiments but this may not only be due to previous overestimates of the thermal conductivity of the window material, but also to the small time scales in shock experiments possibly causing overshoot and non-equilibrium. Boness & Brown (1993) showed that the Hugoniot for solid KBr overshoots the melting curve by almost

1000 K in the 300 kbar region. If we assume a similar overshoot for iron, and given the large uncertainties in the calculation of shock temperatures, one can easily reconcile the phase diagram measured by Boehler (1993) to 2 Mbar with the sound velocity measurements made during shock by Brown & McQueen (1986).

For clarification of the phase diagram of iron, more experimental data are clearly needed, such as more precise diamond-cell work on the solid–solid transitions, especially the $\epsilon$–$\theta$ transition to at least 2 Mbar. Shock-wave experiments on heated iron would provide a check on the problem of overshoot because then the Hugoniot would cross the melting curve at lower pressures, where most measurements are in very good agreement with each other. Synchrotron X-ray experiments on laser-heated iron samples will provide the necessary information on the volumes at high $P$–$T$ conditions to construct phase diagrams in a $P$–$V$–$T$ space.

## 3. Effect of light elements on the melting temperature of iron

The nature of the light component required for the outer core to satisfy density arguments is unknown. Any combination of silicon, oxygen, sulphur, carbon and hydrogen is possible, but most studies have favoured oxygen and sulphur. At ambient conditions, the addition of a small amount of light elements depresses the melting temperature of iron up to a few hundred degrees due to eutectic behaviour. Data at high pressure, however, are scarce and are limited to 150 kbar in the Fe–FeO–FeS system (Urakawa *et al.* 1987; Usselman 1975). Additionally melting in these studies was not detected *in situ*, but relied on the interpretation of textural changes in the sample upon quenching. Urakawa *et al.* (1987) measured two melting temperatures in the Fe–O–S, and in the Fe–Ni–O–S systems (at 60 and 150 kbar) and concluded from their data that the melting temperature of the core-forming material at the core–mantle boundary pressure may be around 1800 K. This is difficult to reconcile with estimates of the core–mantle boundary temperature and the adiabatic temperature rise in the outer core. Stevenson (1981) calculated a melting point depression of iron with 8% sulphur of 1100 K from an estimate of the entropy of melting.

Using similar techniques as for his iron melting experiments, Boehler (1992) measured the melting curves of FeO and FeS to about 0.5 Mbar, and mixtures of Fe and FeO to 1.6 Mbar (Boehler 1993). For all compounds, the melting temperatures measured in the diamond cell are in excellent agreement with previous low-pressure measurements using conventional methods. For the Fe–FeO mixtures, the melting depression observed at low pressures diminished at higher pressures. New, previously unpublished data on a mixture of 70% Fe, 20% FeO, and 10% FeS to 0.5 Mbar, showed the same trend. At low pressure, the solidus temperature in a multicomponent system can be easily detected visually by observing liquid motion of a matrix containing solid particles if the heated portion is relatively large compared to the particle size. At higher pressures, however, the hotspot becomes smaller due to an increase in the thermal conduction within the pressure chamber. This makes the detection of the solidus temperature more difficult, resulting in larger error bars. The data, however, suggest that one can preclude the previously predicted large melting depression of iron for the light elements sulphur and oxygen. The data are summarized in figure 4. The melting curves of the end-members Fe, FeO and FeS, and the mixtures in the Fe–O–S system show similar trends in their pressure dependence, but the melting curves converge instead of diverge, as previously assumed. At 0.5 Mbar the difference in the melting temperatures is only a few hundred degrees.




PHILOSOPHICAL TRANSACTIONS OF THE ROYAL SOCIETY A MATHEMATICAL, PHYSICAL & ENGINEERING SCIENCES

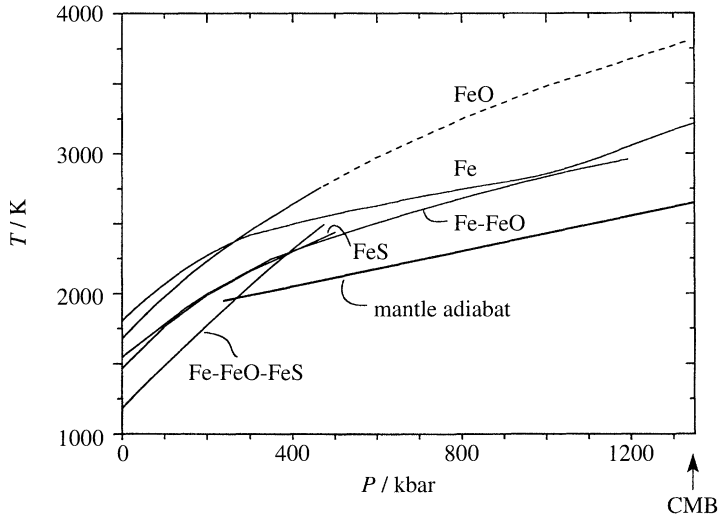


Figure 4. Melting of the Fe–O–S system in relation to a possible geotherm.

## 4. Temperature at the inner-core boundary

The temperature at the inner-core boundary may be found by extrapolating the melting curve of iron, as shown in figure 2. This, however, requires a number of assumptions.

(1) Light elements do not change the melting temperature of pure iron at very high pressure by more than what is shown in figure 4. This implies that the Fe–O–S system might behave like a solid solution system rather than a eutectic system. If, however, all the above compounds melt at the same temperature at the inner-core boundary, the inner core must have the same composition as the outer core. Then the density increase estimated from seismic observations at the inner-core boundary of *ca.* 0.5 g cc$^{-1}$ (or about 4%) (Masters & Shearer 1990) must be due to freezing only. Such a large volume change due to freezing, however, seems rather unlikely. Additionally, gravitational energy release associated with the upward redistribution of the light elements in the outer core would then not be available to generate the Earth's magnetic field, and the single source of energy to drive the dynamo would have to be the latent heat of freezing of iron at the inner-core–outer-core boundary.

(2) Shock-wave temperature measurements have to be disregarded because they would require an additional triple point between 2 and 3.3 Mbar. Such a triple point would deflect the melting curve upwards (Anderson 1994) leading to a melting temperature of iron at the inner-core boundary which is at least 1500 K higher than the present estimate. Such an additional triple point, however, is difficult to reconcile with the recent observation of a solid–solid transition in diamond-cell experiments.

These melting results are important for models on core formation. As shown in figure 2, the melting curves of iron and its compounds are nearly parallel and about 500 K above the present-day geotherm of the lower mantle. Here, the geotherm is assumed purely adiabatic with a fixed temperature at 660 km depth of 1950 K, which is the transition temperature of (Mg,Fe)$SiO_3$-perovskite at the equivalent pressure, obtained from $CO_2$-laser-heating experiments in the diamond cell (Boehler & Chopelas 1991). At the time of core formation, mantle temperatures were a few hundred degrees higher than today and probably exceeded the melting curves of the iron compounds

shown in figure 4. Thus, the core could have formed by a simple physical mechanism in the early history of the Earth when iron and its compounds were molten. This does not require eutectic behaviour, miscibility of iron and its compounds, or special compositions for the core material.

## 5. Melting of the major mantle materials (Mg,Fe)$SiO_3$-perovskite and (Mg,Fe)O-magnesiowüstite

If the lower mantle has the same chemical composition as the upper mantle, it will be composed of about 70% (Mg,Fe)$SiO_3$-perovskite and about 20% (Mg,Fe)O-magnesiowüstite. High-pressure mineral physics data are yet too imprecise to estimate exact densities of these minerals at lower mantle conditions and the seismically derived densities are too inaccurate to constrain an exact mineral composition of the lower mantle by density arguments (Chopelas & Boehler 1992). If both of the above phases are coexistent in the lower mantle, (Mg,Fe)O-magnesiowüstite is most likely iron enriched compared to (Mg,Fe)$SiO_3$-perovskite with Mg-numbers of 92 and 84, respectively (Kesson & Fitz Gerald 1992).

The melting temperature of the lower mantle is assumed to be near the eutectic temperature in the phase diagram MgO–FeO–$SiO_2$. This eutectic temperature has to be above the mantle geotherm because there is no indication of extensive melting in the lower mantle from seismic observation. For the MgO–$SiO_2$ system, it has been suggested previously (Ito & Takahashi 1989) that $MgSiO_3$-perovskite lies near the eutectic composition, and this requires higher melting temperatures for the end-members MgO and $SiO_2$. Previous estimates of the melting curves of both end-members from theory and shock data (Gong *et al.* 1991; Jackson 1977; Lyzenga *et al.* 1983) suggested a strong increase in the melting temperatures with pressure, whereas previous melting measurements in laser-heated diamond-anvil cells on (Mg,Fe)$SiO_3$-perovskite (see, for example, Sweeney & Heinz 1993) showed very shallow melting curves with large inconsistencies in the melting slopes. Because of these inconsistencies, and because the pressure dependence of melting of MgO had not been measured previously, Zerr & Boehler (1993, 1994) measured the melting curves of MgO and (Mg,Fe)$SiO_3$-perovskite with improved laser-heating techniques to find an upper bound for the melting temperature in the lower mantle.

### (*a*) (Mg,Fe)$SiO_3$-*perovskite*

Due to its primary role in the lower mantle, a significant number of both theoretical and experimental studies can be found in the literature (Zerr & Boehler 1993). Melting temperatures at the base of the mantle from theoretical and experimental estimates range from about 2500 to 8000 K. Previous measurements (Sweeney & Heinz 1993) suggested very low melting temperatures of (Mg,Fe)$SiO_3$-perovskite in the lower mantle. These results, however, were subject to large systematic errors, mainly due to temperature gradients in the diamond cell and other imperfections in the detection of melting and in the temperature measurement. Newer measurements (Zerr & Boehler 1993), using significantly different technology, resulted in a melting curve of (Mg,Fe)$SiO_3$-perovskite that is much higher than all previous measurements with extrapolated melting temperatures at the base of the mantle exceeding 7000 K. Such large discrepancies among experimental results are often interpreted as random uncertainties based on intrinsic difficulties in these complicated experiments. Here, I want to emphasize the importance of technical improvements designed to remove

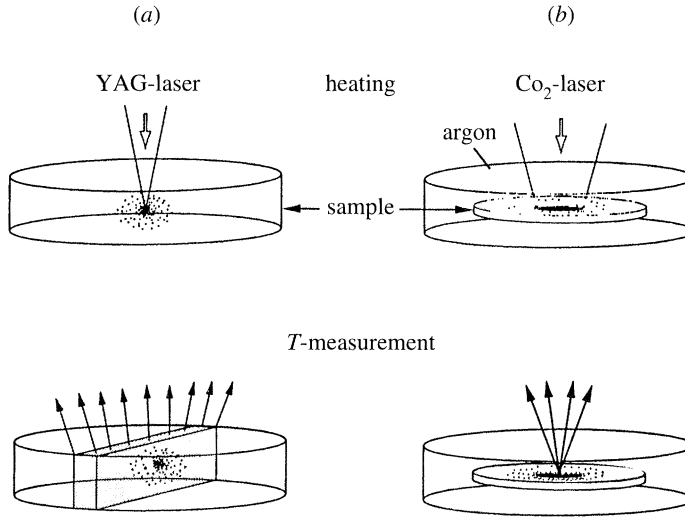


Figure 5. Two different methods to heat minerals and measure temperatures in the diamond cell. The large disc represents the pressure chamber. (*a*) shows the method used earlier (Heinz & Jeanloz 1987; Knittle & Jeanloz 1989; Sweeney & Heinz 1993) compared to (*b*) the method used by Zerr & Boehler (1993, 1994).

large systematic errors by comparing the two different laser-heating techniques used to measure melting of Mg-Si-perovskite.

Before our own measurements, three measurements were reported in the literature (Heinz & Jeanloz 1987; Knittle & Jeanloz 1989; Sweeney & Heinz 1993), all of which used identical laser-heating techniques. Schematics are shown in figure 5. In these experiments, the entire pressure chamber was filled with the powdered sample, which acted as its own pressure medium (figure 5*a*). A Nd:Yag laser ($\lambda = 1.06\,\mu$m) was used to heat the sample. The wavelength of this laser is unsuitable to heat iron-free silicates and its radiation was only weakly absorbed by samples containing a small amount of iron. This required tight focussing of the laser beam which created an extremely small hotspot. Due to the high thermal conduction of the sample, and even more, of the diamond anvils, the hottest portion of the sample is located somewhere in the centre of the sample. It is physically impossible to measure the temperature in the centre of such a hotspot because the emission spectrum is some average of the entire temperature range. Calculation of peak temperatures is exceedingly difficult because of the extreme temperature gradients in all three dimensions. With regards to radial temperature gradient, the optical arrangement used by these authors only allowed the measurement of emitted light from volumes many hundred times larger than the melted volume of the sample (see figure 5). Temperatures reported from such measurements therefore have to be considered as average temperatures of the heated sample volume, which are substantially below the peak temperature. At higher pressures, temperature gradients in the laser-heated diamond cell increase strongly, thus increasing this systematic error.

Temperature gradients in our own experiments (Zerr & Boehler 1993) were significantly reduced in both the axial and radial direction, thus eliminating previous problems in the temperature measurement. Thin sample discs (less than 10 $\mu$m) were thermally insulated from the diamond anvils by argon, which neither absorbs laser radiation nor emits incandescent light. This eliminated axial temperature gra-

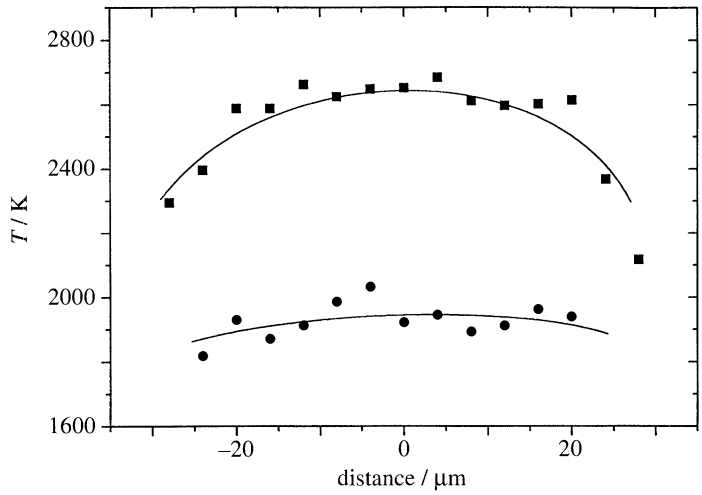


Figure 6. Temperature profiles measured at two different temperatures on thin discs of (Mg,Fe)$SiO_3$-perovskite shown on figure 5*b*. $P = 287$ kbar.

dients. $CO_2$-laser radiation ($\lambda = 10.6$ μm) was used, which is almost fully absorbed by silicates with a power about eight times higher than that of YAG-lasers. This allowed defocussed laser beams to heat the sample (figure 5*b*) and thus reduced radial temperature gradients. Temperatures were directly measured from small spots using pinhole apertures which allowed the direct measurement of peak temperatures and temperature gradients. Figure 6 shows two temperature profiles at two different sample temperatures measured across the sample in 3 μm steps from areas with 3 μm in diameter.

The melting temperatures by Zerr & Boehler (1993) were determined by measuring peak temperatures *in situ* while the laser-power was slowly increased. As soon as the sample melted, the laser absorption increased drastically. The melting temperatures reported are the last temperatures of the solid before the sample melted.

### (*b*) MgO *and* (Mg,Fe)O-*magnesiowüstite*

Using identical techniques as for (Mg,Fe)$SiO_3$-perovskite, Zerr & Boehler (1994) measured the pressure dependence of melting of MgO for the first time. These measurements to 315 kbar yielded a rather flat melting curve with a slope at one atmosphere of 3.5 K kbar$^{-1}$, as compared to 11 K kbar$^{-1}$ estimated by Jackson (1977), which was based on elastic shear instability and analogy with LiF. Even steeper melting curves were predicted from molecular dynamics calculations (Gong *et al.* 1991). In order to check the effect of iron on the melting behaviour of MgO, a melting temperature of $(Mg_{0.85}Fe_{0.15})$O-magnesiowüstite of $3400 \pm 100$ K was measured in an argon pressure medium at 182 kbar using a YLF-laser ($\lambda = 1.05$ μm) and methods described elsewhere (Boehler 1992). The previously measured melting curve of FeO (Boehler 1992) is nearly parallel to the melting curve of MgO and the melting temperature of magnesiowüstite is in perfect agreement with the melting behaviour of a solid solution system between MgO and FeO.

Figure 7 shows extrapolated melting temperatures to the pressure of the core–mantle boundary using the Lindemann formula. For MgO this yields melting temperatures at the bottom of the lower mantle of slightly above 5000 K, provided that there are no phase transitions in this pressure range. A linear $T_m$ versus com-

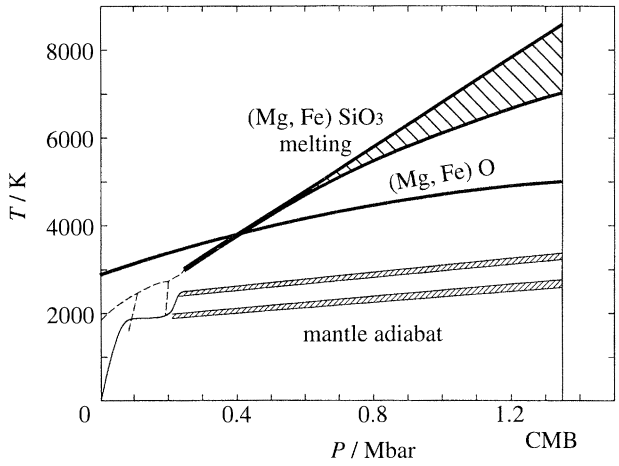


Figure 7. Melting curves of (Mg,Fe)$SiO_3$-perovskite and (Mg,Fe)O-magnesiowüstite extrapolated to the core–mantle boundary in comparison to two possible mantle geotherms.

pression relationship yields nearly identical results. Our estimated melting curve of (Mg,Fe)O-magnesiowüstite crosses the melting curve of (Mg,Fe)$SiO_3$-perovskite at about 430 kbar. This implies that the MgO-$SiO_2$ phase diagram changes substantially at higher pressures and is quite different from that suggested by Ito (1989).

## 6. Geophysical and geochemical consequences

Our melting data on (Mg,Fe)$SiO_3$-perovskite and on (Mg,Fe)O-magnesiowüstite suggest that the solidus of the lower-mantle material is about twice as high as the present average mantle temperature. This means that the mantle was solid throughout the geologic history of the Earth and chemical partitioning processes which require melting or partial melting most likely did not occur. A magma ocean could not have been much deeper than about 700 km because, below this depth, (Mg,Fe)$SiO_3$-perovskite is the stable phase with a melting curve that rapidly diverges from the nearly adiabatic average geotherm.

Based on the high melting temperatures of (Mg,Fe)$SiO_3$-perovskite in the lower mantle, a strong increase in the viscosity was recently predicted (van Keken *et al.* 1994). This suggested a rather passive role of the lower mantle in large-scale deformation. The addition of (Mg,Fe)O-magnesiowüstite most likely lowers the viscosity because it possesses entirely different rheological properties than (Mg,Fe)$SiO_3$-perovskite and has significantly lower melting temperatures.

The actual temperature distribution in the lower mantle might deviate significantly from adiabatic conditions (Yuen *et al.* 1993) based on the observed lateral variations in the sound velocities from seismic tomography and laboratory data on the pressure dependence of thermal expansivity and sound velocity. In the centre of plume heads, temperatures may be 1000–1500 K higher than the average mantle temperature. Such large temperature variations are possible in view of the high melting temperatures of the lower mantle materials. For the same reason, the region D″ at the very bottom of the mantle may be interpreted as a thermal boundary layer with temperature jumps in excess of 1000 K without limitations from mantle melting arguments. The temperature jump across the core–mantle boundary, estimated from the melting experiments on iron and its oxygen and sulphur compounds described above, is at

least 1300 K but could be as high as 2000 K. Such large temperature variations over a relatively small depth range could explain the change in the observed seismic properties.

I thank A. Chopelas and A. Zerr for their help in preparing this manuscript.

## References

Anderson, O. L. 1994 Imperfections in the 1993 phase diagram of iron. In *High-pressure science and technology—1993* (ed. S. Schmidt, J. Shaner, G. A. Samara & M. Ross), pp. 907–910. New York: American Institute of Physics.

Boehler, R. 1986 The phase diagram of iron to 430 kbar. *Geophys. Res. Lett.* **13**, 1153-1156.

Boehler, R. 1992 Melting of the Fe–FeO and the Fe–FeS systems at high pressure: constraints on core temperatures. *Earth Planet. Sci. Lett.* **111**, 217–227.

Boehler, R. 1993 Temperatures in the Earth's core from melting-point measurements of iron at high static pressures. *Nature* **363**, 534–536.

Boehler, R. & Chopelas, A. 1991 A new approach to laser heating in high pressure mineral physics. *Geophys. Res. Lett.* **18**, 1147–1150.

Boehler, R. & Chopelas, A. 1992 Phase transitions in a 500 kbar–3000 K gas apparatus. In *High-pressure research: application to Earth and planetary sciences* (ed. Y. Syono & M. H. Manghnani), pp. 55–60. Washington, DC: American Geophysical Union.

Boehler, R., von Bargen, N. & Chopelas, A. 1990 Melting, thermal expansion, and phase transitions of iron at high pressures. *J. Geophys. Res.* **95**, 21 731–21 736.

Boness, D. A. & Brown, J. M. 1993 Bulk superheating of solid KBr and CsBr with shock waves. *Phys. Rev. Lett.* **71**, 2931–2934.

Brown, J. M. & McQueen, R. G. 1986 Phase transitions, Grüneisen parameter and elasticity for shocked iron between 77 GPa and 400 GPa. *J. Geophys. Res.* **91**, 7485–7494.

Chopelas, A. & Boehler, R. 1992 Thermal expansivity in the lower mantle. *Geophys. Res. Lett.* **19**, 1983–1986.

Duba, A. 1992 Earth's core not so hot. *Nature* **359**, 197–198.

Duba, A. 1994 Iron—what is melt? In *High-pressure science and technology—1993* (ed. S. Schmidt, J. Shaner, G. A. Samara & M. Ross), pp. 923–926. New York: American Institute of Physics.

Gallagher, K. G. & Ahrens, T. G. 1994 First measurements of thermal conductivity in griceite and corundum at ultra high pressure and the melting point of iron. *EOS* **75**, 653.

Gong, Z., Cohen, R. E. & Boyer, L. L. 1991 Molecular dynamics simulations of melting of MgO at high pressures. Annual report, Director Geophysics Laboratory, Carnegie Institute, Washington, pp. 129–134.

Heinz, D. & Jeanloz, R. 1987 Measurement of the melting curve of $Mg_{0.9}Fe_{0.1}SiO_3$ at lower mantle conditions and geophysical implications. *J. Geophys. Res.* **92**, 11 437–11 444.

Ito, E. & Takahashi, E. 1989 Postspinel transformations in the system $Mg_2SiO_4$–$Fe_2SiO_4$ and some geophysical implications. *J. Geophys. Res.* **94**, 10 637–10 646.

Jackson, I. 1977 Phase relations in the system LiF–$MgF_2$ at elevated pressures: implications for the proposed mixed-oxide zone of the Earth's mantle. *Phys. Earth Planet. Inter.* **14**, 86–94.

Kesson, S. E. & Fitz Gerald, J. 1992 Partitioning of MgO, FeO, NiO, MnO, and $Cr_2O_3$ between magnesium silicate perovskite and magnesiowüstite: implications for the origin of inclusions in diamond and the composition of the lower mantle. *Earth Planet. Sci. Lett.* **111**, 229–240.

Knittle, E. & Jeanloz, R. 1989 Melting curve of (Mg,Fe)$SiO_3$ perovskite to 96 GPa: Evidence for a structural change in lower mantle melts. *Geophys. Res. Lett.* **16**, 421–424.

Liu, L. G. & Bassett, W. A. 1975 The melting curve of iron up to 200 kbar. *J. Geophys. Res.* **80**, 3777–3782.

Lyzenga, G. A., Ahrens, T. J. & Mitchell, A. C. 1983 Shock temperatures of $SiO_2$ and their geophysical implications. *J. Geophys. Res.* **88**, 2431–2444.





PHILOSOPHICAL TRANSACTIONS OF THE ROYAL SOCIETY A MATHEMATICAL, PHYSICAL & ENGINEERING SCIENCES

Masters, T. G. & Shearer, P. M. 1990 Summary of seismological constraints on the structure of the Earth's core. *J. Geophys. Res.* **95**, 21 691–21 695.

Ming, L. C. & Bassett, W. A. 1974 Laser heating in the diamond anvil press up to 2000 °C sustained and 3000 °C pulsed at pressures up to 260 kilobars. *Rev. Scient. Instrum.* **9**, 1115–1118.

Ringwood, A. E. & Hibberson, W. 1990 The system Fe–FeO revisited. *Phys. Chem. Miner.* **17**, 313–319.

Saxena, S. K., Shen, G. & Lazor, P. 1993 Experimental evidence for a new iron phase and implications for the Earth's core. *Science* **260**, 1312–1314.

Saxena, S. K., Shen, G. & Lazor, P. 1994 Temperatures in earth's core based on melting and phase tranformation experiments on iron. *Science* **264**, 405–407.

Shen, G., Lazor, P. & Saxena, S. K. 1993 Melting of wüstite and iron up to pressures of 600 kbar. *Phys. Chem. Minerals* **20**, 91–96.

Stevenson, D. J. 1981 Models of the Earth's core. *Science* **214**, 611–619.

Sweeney, J. S. & Heinz, D. L. 1993 Melting of iron–magnesium–silicate perovskite. *Geophys. Res. Lett.* **20**, 855–858.

Urakawa, S., Kato, M. & Kumazawa, M. 1987 Experimental study of the phase relation in the system Fe–Ni–O–S up to 15 GPa. In *High-pressure research in mineral physics* (ed. M. H. Manghnani & Y. Syono), pp. 95–111. Tokyo: Terra.

Usselman, T. M. 1975 Experimental approach to the state of the core: part II. Composition and thermal regime. *Am. J. Sci.* **275**, 291–303.

van Keken, P. E., Yuen, D. A. & van den Berg, A. P. 1994 Implications for mantle dynamics from the high melting temperatures of perovskite. *Science* **264**, 1437–1439.

Williams, Q. R., Jeanloz, R., Bass, J., Swendsen, B. & Ahrens, T. J. 1987 The melting curve of iron to 2.5 Mbar: a constraint on the temperature in the Earth's core. *Science* **236**, 181–182.

Yoo, C. S., Akella, J. & Ruddle, C. 1992 Melting studies of iron and uranium by DAC: laser heating experiments. *EOS* **73**, 64.

Yoo, C. S., Holmes, N. C., Ross, M., Webb, D. J. & Pike, C. 1993 Shock temperatures and melting of iron at earth core conditions. *Phys. Rev. Lett.* **70**, 3931–3934.

Yuen, D. A., Cadek, O., Chopelas, A. & Matyska, C. 1993 Geophysical inferences of thermal–chemical structures in the lower mantle. *Geophys. Res. Lett.* **20**, 889–902.

Zerr, A. & Boehler, R. 1993 Melting of (Mg,Fe)$SiO_3$-perovskite to 625 kbar: indication of a high melting temperature in the lower mantle. *Science* **262**, 553–555.

Zerr, A. & Boehler, R. 1994 Constraints on the melting temperature of the lower mantle from high-pressure experiments on MgO and magnesiowüstite. *Nature* **371**, 506–508.





PHILOSOPHICAL TRANSACTIONS OF THE ROYAL SOCIETY A MATHEMATICAL, PHYSICAL & ENGINEERING SCIENCES